Effect of Modifiers on Morphology and Thermal Properties of Novel Thermoplastic Polyurethane-Peptized Laponite Nanocomposite

Ananta K. Mishra, Santanu Chattopadhyay, Golok B. Nando

Rubber Technology Center, Indian Institute of Technology Kharagpur, Kharagpur 721 302, India

Received 28 November 2008; accepted 17 June 2009
DOI 10.1002/app.30975
Published online 8 September 2009 in Wiley InterScience (www.interscience.wiley.com).

ABSTRACT: Laponite RDS (Laponite containing pyrophosphate based peptizer) was modified with cetyl trimethyl ammonium bromide (cLS) and dodecylamine hydrochloride (dLS), respectively. Thermoplastic polyurethane (TPU)-modified Laponite RDS nanocomposites were prepared by solution mixing technique. Morphologies of these two modified clay-nanocomposites are found to be markedly different. cLS based TPU nanocomposites exhibit partly exfoliated, intercalated, and aggregated structure at lower clay content but a network type of structure is observed at higher clay content. However, dLS based TPU nanocomposites demonstrate spherical cluster type of structure at all clay contents. Nearly two fold increase in storage modulus is observed in both glassy and rubbery state with merely 1% cLS content which gradually decreases with an increase in the clay content. However, in case of dLS filled nanocomposite, gradual increase in storage modulus is observed with an increase in the clay content. Thermogravimetric analysis (TGA) studies indicate that the temperature corresponding to 5 wt % degradation of TPU is enhanced by 19.1 and 12.5°C with the addition of merely 1% cLS and dLS, respectively. However, the activation energy of degradation of neat TPU, as determined by isothermal TGA analysis, is found to be higher than that of the nanocomposites containing 1% of cLS and dLS, respectively. © 2009 Wiley Periodicals, Inc. J Appl Polym Sci 115: 558–569, 2010

Key words: polyurethanes; peptized Laponite; nanocomposites; thermal properties; dynamic mechanical properties

INTRODUCTION

Thermoplastic polyurethane (TPU) is used in many engineering and biomedical applications. This is possible because of its inherent higher mechanical strength, excellent abrasion resistance, ease in processing, and biocompatibility. However, TPUs have certain limitations like inadequate thermal stability and flame retardancy. These restrict its end use in certain areas, especially in space applications. In industries, the most commonly used flame retardants are halogen based. However, these compounds liberate toxic gases during combustion which limit their applications. In this regard, nanofillers especially nanoclay in the polyurethane (PU) matrix are considered as potential alternatives to overcome this problem.[1] This is because of the manifold increase in the property spectrum of the nanocomposites when compared with the neat polymers. Additionally, the nanoclays enhance the thermal stability, flame retardancy, and barrier properties of TPU matrix.[2–7]

As reported earlier by Saunders et al.,[8] the degradation of urethane linkage can follow four types of reaction pathways as shown in Scheme 1. The degradation of PUs yields a complex mixture of products which is often very difficult to correlate precisely with the basic degradation mechanism. However, primarily degradation follows a depolycondensation process (first mechanism in Scheme 1).[9–11]

In earlier publications, the authors[12,13] have reported that colloidal suspension of Laponite RD (L) modified with dodecylamine hydrochloride and cetyltrimethyl ammonium bromide in tetrahydrofuran (THF) were not stable for long time. Still then their reinforcing effect in the TPU matrix was observed to a significant extent. However, it is well established that nanocomposites display better property spectrum, when fillers are uniformly dispersed in the matrix. To improve the dispersion of the nanoclay further, we have preferred to use Laponite RDS (LS) which provides additional sites for cationic modification with alkyl ammonium ions. Interestingly, it was observed that LS modified by cetyltrimethyl ammonium bromide was stable for months together in THF. In this work, Laponite RDS (LS) has been used as nanofiller in the TPU matrix.

Correspondence to: G. B. Nando (golokb@rtc.iitkgp.ernet.in).

Contract grant sponsor: ISRO, Bangalore.

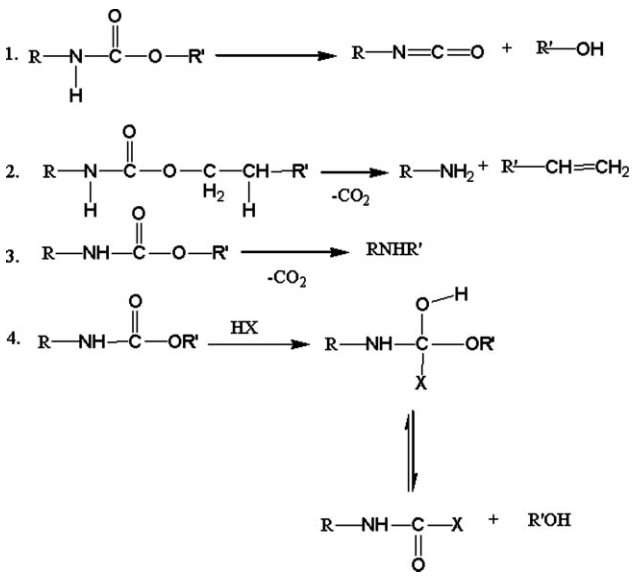

Scheme 1 Degradation mechanisms of urethane linkages.

Laponite RDS is a synthetic hectorite clay with empirical formula $Na_{0.7}(Si_8Mg_{5.5}Li_{0.3})$ O_{20} $(OH)_4$ $Na_4P_2O_7$. It is a peptized version of Laponite RD. The *peptizer* sodium pyrophosphate ($Na_4P_2O_7$) is adsorbed on the clay mineral for enhancing the dispersion of Laponite in highly polar solvents including in the aqueous media. It has the advantage of high purity and transparency and can be used in highly polar polymers like polyethylene oxide in pristine form. It has well-controlled dimensions (disc shaped particles of mean diameter of 30 nm and thickness 1 nm) that does not form the strongly layered structures common in natural clay.[14,15] The excess negative charge originated due to the nonstoichiometric cation distribution is compensated by Na^+ ions located in the intergallery space between the silicate layers. Adsorbed $Na_4P_2O_7$ on the surface of LS is expected to provide additional sodium ions for replacement by the cation exchange during modification. Thus, we expect that the alkyl ammonium pyrophosphate (after modification) would give rise to additional interaction with TPU matrix when compared with modified Laponite RD. There is no report published in literature dealing with the use of LS in TPU matrix. However, it is well known that phosphorous containing compounds impart enhanced flame resistance to polymer matrices. Hence, it is also expected that modified LS would provide additional flame retardancy to the TPU matrix along with the thermal stability.

This article primarily focuses on the correlation between the morphological and thermal properties of polyurethane clay nanocomposite (TPUCN) prepared by solution mixing technique with LS modified by two different types of surfactants, namely cetyltrimethyl ammonium bromide (c) and dodecyl ammonium hydrochloride (d).

EXPERIMENTAL

Materials

Desmopan KU2 8600E (with a specific gravity of 1.11, which is a polyether based TPU prepared from MDI and polytetramethylene glycol chain extended with 1,4-butanediol containing 25% hard segment) used in this work was kindly supplied by M/S Bayer Materials Science Ltd., Chennai, India. Laponite RDS (supplied by Rockwood additives Ltd., UK) was used as received. Dodecyl amine and cetyl trimethyl ammonium bromide were procured from Sigma-Aldrich (St. Louis, MO) and used without further purification. THF and concentrated hydrochloric acid (Reagent Grade, Merck, KGaA, Darmstadt, Germany) were used without any further purification.

Modification of clay

The inorganic clay Laponite RDS (LS) was modified with cetyl trimethyl ammonium bromide (c) and dodecyl ammonium chloride (d), respectively by using the standard ion exchange process[14] to increase the interaction between the hydrophobic polymer and the hydrophilic clay. The organic-modification also helps to increase the interlayer spacing of the clay. The amount of surfactant required for the cation exchange is calculated by using eq. (1):

$$\text{Amount of surfactant} = \frac{5.6 \times 1.2}{31 \times 100} \times WM \qquad (1)$$

where 5.6 is the percentage of Na_2O present, 1.2 is the number of equivalents of surfactant taken, 31 is the equivalent weight of the replaceable sodium ion present, W is the amount of clay in grams to be modified, and M is the molecular weight of the surfactant. Clay modified with "c" and "d" would be designated here onwards as "cLS" and "dLS," respectively.

Preparation of nanocomposites

A 20% solution of TPU was first prepared in THF solvent. Calculated amount of dLS or cLS was mixed with THF and stirred under ultrasonic vibration for 30 min and then added slowly to the TPU solution, maintaining gentle stirring. Stirring continued further for 15 min. The mixture was then sonicated for 15 min to make homogeneous dispersion of clay in the polymer matrix. It was then casted on a petridish and allowed the solvent to evaporate slowly at room temperature. After complete removal of the

TABLE I
Nomenclature of Modified Clay and TPUCN

Designation	Details	Designation	Details
cLS	Laponite RDS modified by cetyl trimethyl ammonium bromide	dLS	Laponite RDS modified by dodecyl amine hydrochloride

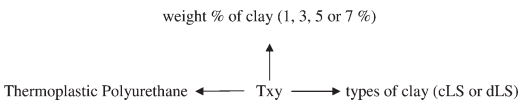

Example: T0, TPU with 0 % clay; T1cLS, TPU with 1% of cLS; T5dLS, TPU with 5% of dLS.

solvent at room temperature, sample was kept in a vacuum oven at 70°C till constant weight. Control PU sample was prepared by following the same procedure excluding the addition of clay to accomplish a better comparison. Nanocomposite so prepared by using LS modified with two different types of surfactants would be referred here onwards as T*xy*, where, *x* and *y* stands for weight percentage of clay used and type of clay used (cLS or dLS), respectively. The nomenclature of the modified clay and TPUCN are given in Table I.

CHARACTERIZATION

Fourier transform infrared (FTIR) studies were performed on a PerkinElmer FTIR spectrophotometer from 4000 to 400 cm^{-1}. Wide angle XRD (WAXRD) in the lower angular range (2θ value 2–10°) was performed using a Phillips Pan analytical X-ray diffractometer (model: XPert Pro, The Netherlands) equipped with Cu target (CuKα) and Ni filter. Transmission electron microscopy (TEM) was performed in a high resolution TEM of JEOL JEM 2100 make, Japan, after microtoming the samples (∼ 50 nm section) using LEICA ULTRACUT UCT (Austria) microtome, equipped with a diamond knife. Field emission scanning electron microscopy (FESEM) of Carl Zeiss SMT Pvt. Ltd., Germany make (model: Supra 40) was used to study the bulk morphology (samples prepared by slicing off 20 nm surface layer using the same microtoming apparatus). Atomic force microscope (AFM) analysis was performed by using VEECO instruments: CP II in tapping mode by using the cantilever MMP 11123 on molded samples after removing the surface layer (∼ 2 nm) by microtoming procedure as described earlier at ambient temperature. DSC Q100 V8.1, DMA 2980 V1.7B, and TGA Q50 V6.1of TA instruments make, USA were used for differential scanning calorimetry (DSC), dynamic mechanical analysis (DMA), and thermogravimetric analysis (TGA), respectively. Isothermal TGA (for degradation study) was carried out at three different temperatures, 300, 325, and 350°C. For this study temperature was ramped at 10°C/min up to the required temperature, then it was equilibrated at that temperature and isothermal TGA was run for 60 min span at that particular temperature. In each case, 10 mg of sample was taken for testing.

RESULTS AND DISCUSSION

Fourier transform infrared spectroscopy (FTIR)

FTIR spectra of LS, cLS, and dLS are shown in Figure 1. New peaks in the FTIR spectrum for modified clays are seen at 2927 cm^{-1} corresponding to asymmetric C—H_{str}, at 2855 cm^{-1} corresponding to symmetric C—H_{str} and 1485–1475 cm^{-1} corresponding to C—H_{def} vibration, respectively. These peaks confirm the presence of alkyl amine group in the clay after modification. The occurrence of peaks at 3699 and 3691 cm^{-1} for cLS and dLS, respectively attributed to the N—H_{str} further confirms the presence of alkyl amine group in the modified clay.

Wide angle X-ray diffraction

Figure 2(a,b) displays the WAXRD at lower angular range (2–10° of 2θ value) for clay, neat TPU and TPUCN. After several trials no sharp peak is observed for the unmodified Laponite RDS (LS) corresponding to the interlayer gallery spacing commonly observed with natural hectorite clay like montmorilonite. Similar observation was made for Laponite RD and explained in our earlier communication.[15] A broad band ranging from 2θ value of 4 to 6.6° (corresponding to *d* spacing of 2.2–1.3 nm) is

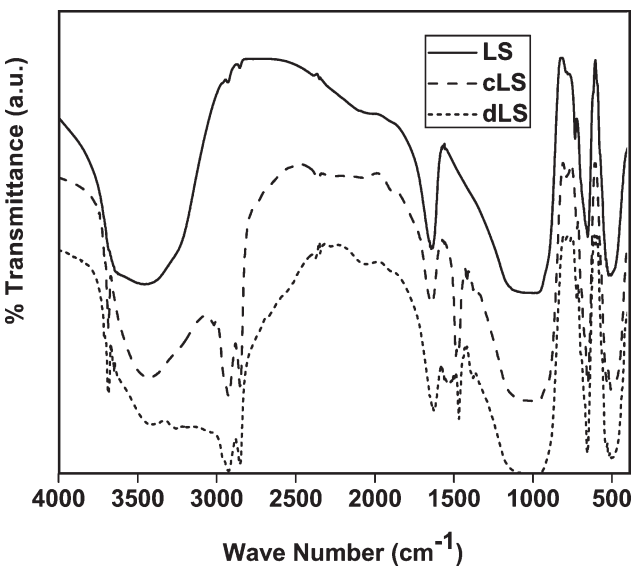

Figure 1 FTIR spectra of unmodified and modified clays.

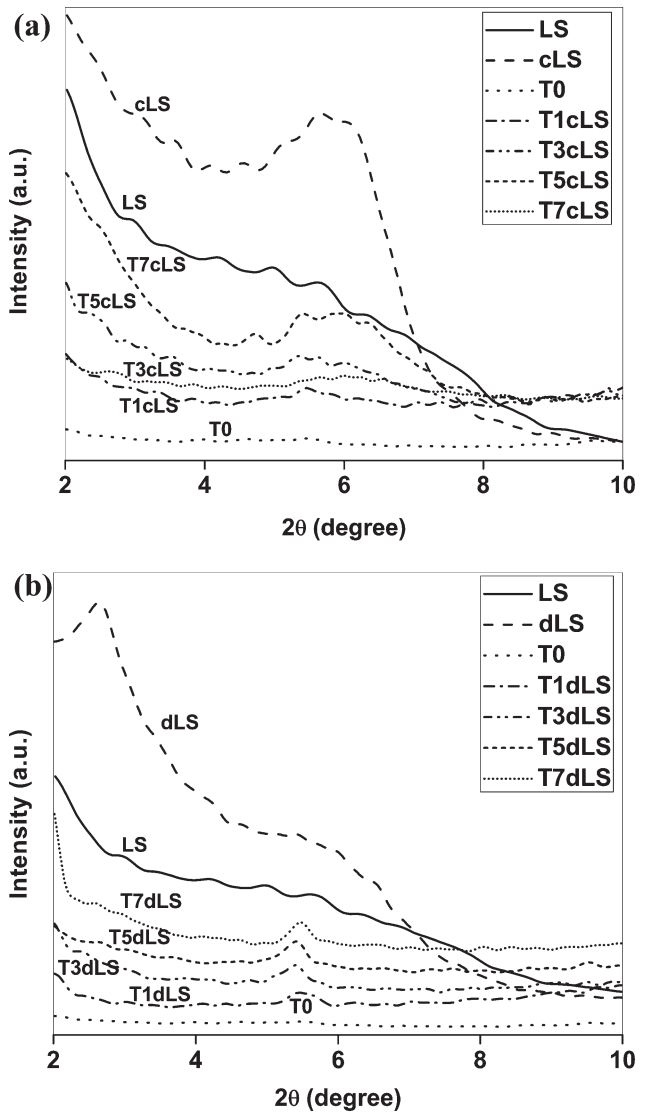

Figure 2 (a) WAXRD of unmodified clay, modified clay, TPU, and TPUCN with cLS and (b) WAXRD of unmodified clay, modified clay, TPU, and TPUCN with dLS.

observed for the modified clay. As reported earlier by Mathias et al.,[16] this may be due to the small diskette size and disordered state of the Laponite clay.

On modification with "c" a broad band ranging from 4.5 to 6.0° 2θ value (comprising of local peaks corresponding to 4.5, 5.1, 5.6, and 6.0° 2θ values) appears in the diffraction pattern. It is observed that TPUCN registers a different type of diffraction pattern at lower clay content than those with higher clay contents. TPUCN with 1% cLS displays a small peak at 5.4° (*d* spacing of 1.6 nm). However, at higher clay content (especially at 5 and 7% clay), the diffraction pattern resembles closely to that of pristine cLS.

Modification of LS with "d" also lead to a broad band in the angular range from 4.8 to 6.5° along with a peak corresponding to 2.6° 2θ value (*d* spacing of 3.4 nm). Addition of dLS into TPU matrix, the broad band present in dLS registers a relatively sharp peak corresponding to ~ 5.4° 2θ value (*d* spacing of 1.6 nm). Interestingly, the peaks retain nearly in the same position for all the clay contents studied here. However, the sharpness of the peaks gradually increases with the increase in clay content. The exact reason for the appearance of the peak corresponding to 2.6° 2θ value (*d* spacing of 3.4 nm) is clearly not known. The possible reason may be due to the increase in gallery spacing of the disordered clay platelets or the formation of secondary aggregate structures. However, this needs further investigation using small angle X-ray or neutron diffraction studies and TEM.

Transmission electron microscopy

Figure 3(a–d) displays the TEM photomicrographs of T1cLS, T5cLS, T1dLS, and T5dLS, respectively. Figure 3(e) displays the TEM photomicrograph of the magnified view of the T5dLS.

T1cLS [Fig. 3(a)] indicates a cylindrical pattern of clay distribution in the TPU matrix. A combination of aggregated, intercalated and partly exfoliated distribution of clay platelets is also seen. Orientations of clay platelets are nearly unidirectional, along with a few randomly oriented contributors. However, at 5% clay content [Fig. 3(b)], cLS forms a network type of structure with increased state of aggregation. Both T1dLS and T5dLS [Fig. 3(c,d)] form nearly similar type of localized spherical aggregation (aggregate size ranging from 150 to 300 nm). In our earlier work,[15] similar types of spherical aggregates were observed when Laponite RD modified with dodecyl ammine hydrochloride was dispersed in the TPU matrix. The composites were well characterized based on the morphology, thermal, and rheological properties. Finally, it was inferred that the modified Laponite RD were located preferentially in the hard domains. The preferential association of Laponite with the more polar hard segment has also been reported earlier by McKinley et al.[17] A magnified view of one of such spherical clusters in T5dLS [Fig. 3(e)] reflects a loose structure accompanied by some comparatively tightly packed aggregates. Presence of the loose structures reveals the fact that TPU is effectively penetrated in to the clay gallery. The tightly packed aggregates possibly correspond to the peak at 5.6° 2θ value, in the X-ray diffractogram. It is interesting to note that, the interplatelet distance within the intercalated structure or loose aggregate ranges from 1.7 to 6.0 nm for cLS and from 8 to 12 nm for dLS, respectively.

Therefore, from TEM analysis, it is apparent that dLS exhibits a preferential association with the hard domains (as the spherical aggregate size matches

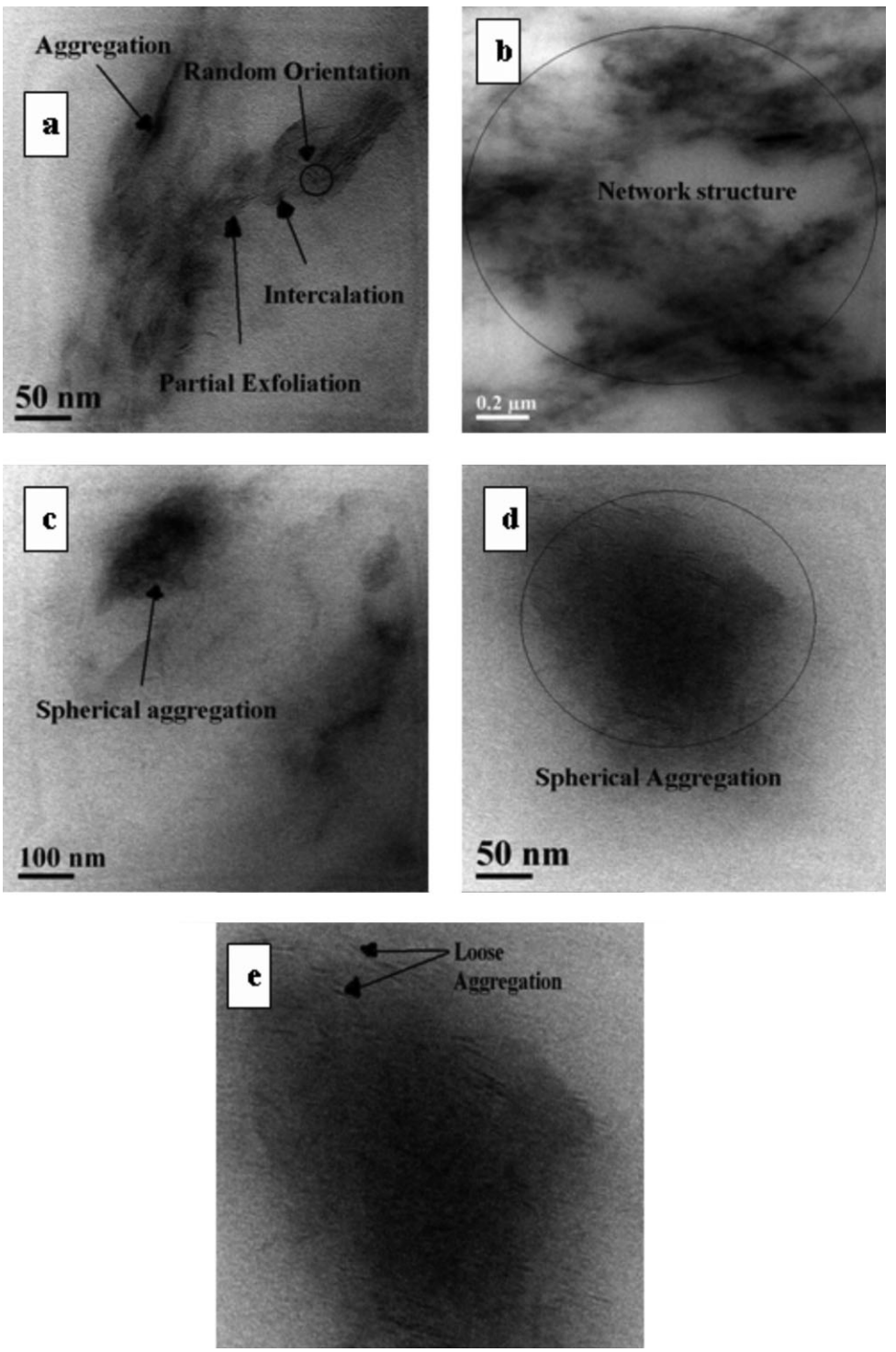

Figure 3 TEM images of T1cLS (a), T5cLS (b), T1dLS (c), T5dLS (d), and magnified view of T5dLS (e).

well with the average size scale of TPU as reported in literature[17]). However, cLS does not show such preference. The greater amount of hard segment (more polar) preference of dLS when compared with cLS can be ascribed due to the more hydrophobic character of dLS when compared with cLS (alkyl chain length of "c" is 16 and that for "d" is 12).

Field emission scanning electron microscopy

Figure 4(a–d) displays the FESEM photomicrograph of T1cLS, T7cLS, T1dLS, and T7dLS, respectively. The small cracks are visible (in all the photomicrographs) due to the nonuniform gold coating and it has been confirmed for all other samples as well.

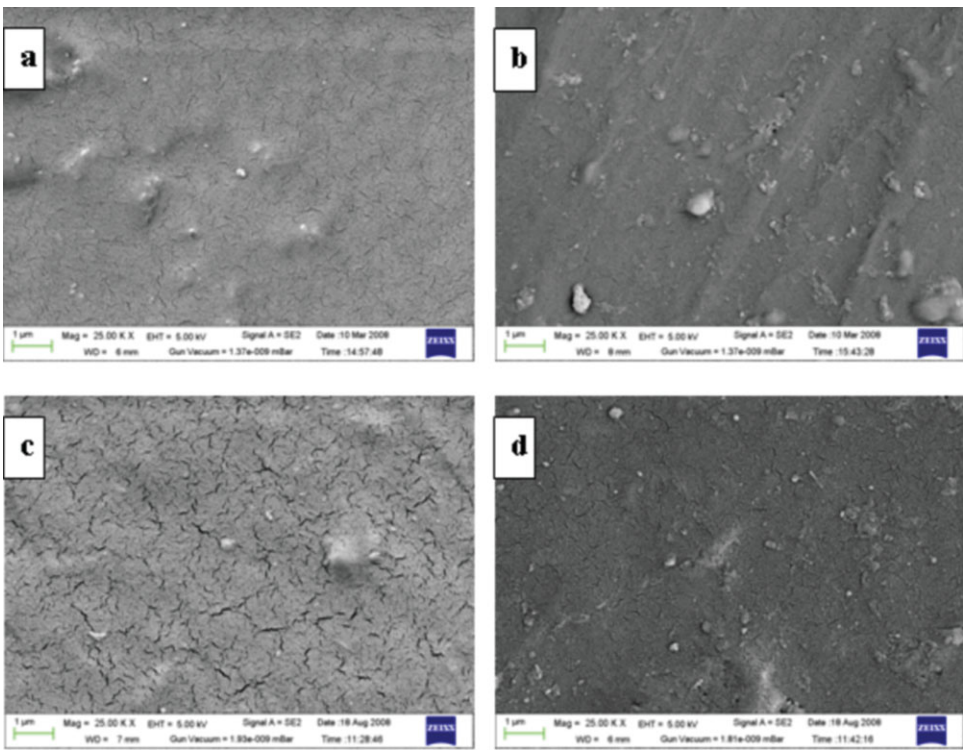

Figure 4 FESEM photomicrographs of T1cLS (a), T7cLS (b), T1dLS (c), and T7dLS (d). [Color figure can be viewed in the online issue, which is available at www.interscience.wiley.com.]

The clay aggregate size varies from 30 to 200 nm for T1cLS [Fig. 4(a)] and 30 to 800 nm for T7cLS [Fig. 4(b)]. Similarly, the aggregate size varies from 30 to 250 nm for T1dLS [Fig. 4(c)] and 30 to 300 nm for T7dLS [Fig. 4(d)]. Hence, increase in clay content increases the size of aggregation in case of cLS based nanocomposite. However, it remains nearly indifferent in case of dLS based nanocomposites. This supports our earlier observations in WAXRD and TEM. More uniform and nanoscale distribution of clay is observed in case of T1cLS when compared with that of T1dLS. However, with increase in clay content, more uniform distribution is noticed in case of T7dLS when compared with that of T7cLS.

Atomic force microscope

Figure 5(a,b) displays the AFM images of T3cLS and T3dLS, respectively. As the samples were microtomed at high speed at room temperature, it is most likely that the soft segments being more elastic when compared with the hard segments would protrude to higher elevation. Gelly type of morphology is seen in both the cases. Partly, these may be due to certain noises or instrumental error. In both images clay platelets seem to be in the aggregated form and bulge outwards from the polymer surface. A comparative study shows that higher aggregation tendency is present in T3cLS when compared with T3dLS. Also, it is observed that in case of T3cLS clay is distributed both in the hard and soft segments (elevated and the depressed part of the sample). However, clay particles are mostly distributed in the hard segment (depressed part of the sample) in case of T3dLS. The uniformity in the aggregation size is also quite prominent in case of T3dLS. These are in line with our earlier observations (refer "Wide angle X-ray diffraction, Transmission electron microscopy, and Field emission scanning electron microscopy" sections).

Differential scanning calorimetry

Figure 6(a,b) displays the DSC thermograms of TPU and TPUCN with different clay contents. The samples sealed inside the aluminium pans were scanned in nitrogen atmosphere at a heating rate of 10°C/min from −75 to 250°C. The thermogram exhibits three endotherms followed by an exotherm. The soft segment T_g appears nearly at −40°C. The endothermic peaks appearing nearly at 98 and 170°C, corresponds to the destruction of the short range and long range ordered hard segment domain (or semicrystalline melting) resulting from enthalpy relaxation.[18–21] Because of the quicker evaporation of the solvent, hard segments are not getting enough time to arrange properly and hence the endotherm from 98 to 170°C is quite broad. After the endotherm an

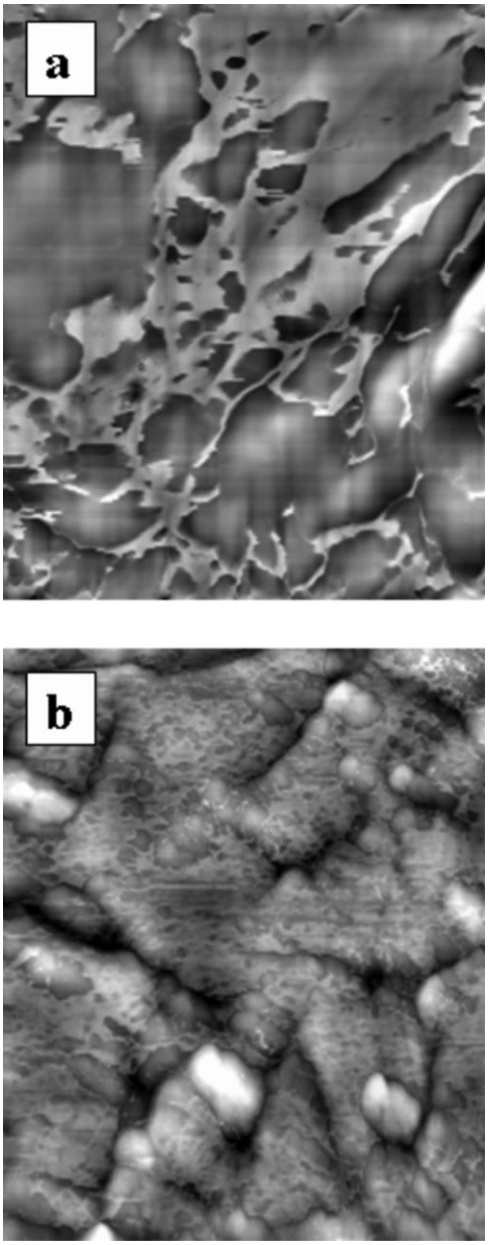

Figure 5 AFM image of T3cLS (a) and T3dLS (b).

exotherm is observed nearly at 200°C corresponding to the degradation of TPU. Hard segment T_g is not clearly seen because of the dominance of the amorphous soft segment over the hard domains and the presence of imperfect crystalline order. There is no significant change in soft segment T_g with the incorporation of nanoclay (Table II). This may be due to the fact that the expected increment in T_g due to the incorporation of clay is being compensated by the plasticizing effect of the unreacted amines present in the modified clays. However, addition of clay increases the sharpness of the endothermic peaks at 98 and 170°C. This suggests that clay modifies the crystalline order in TPU matrix. The endotherms are more distinct and clear in case of cLS based nanocomposites when compared with that of dLS based nanocomposites. The preferential association of dLS with the hard domain (which destroys the crystalline ordering in hard domain) is possibly responsible for this.

Dynamic mechanical analysis

The structure, concentration, and organization of the hard segments and nanoscale distribution and dispersion of clays, have a dominant influence on the physical and mechanical properties of TPU. Figure 7(a,b) represents the change in storage modulus with respect to temperature on neat TPU and TPUCN, respectively. For this study, the samples were subjected to a sinusoidal displacement of 0.1%

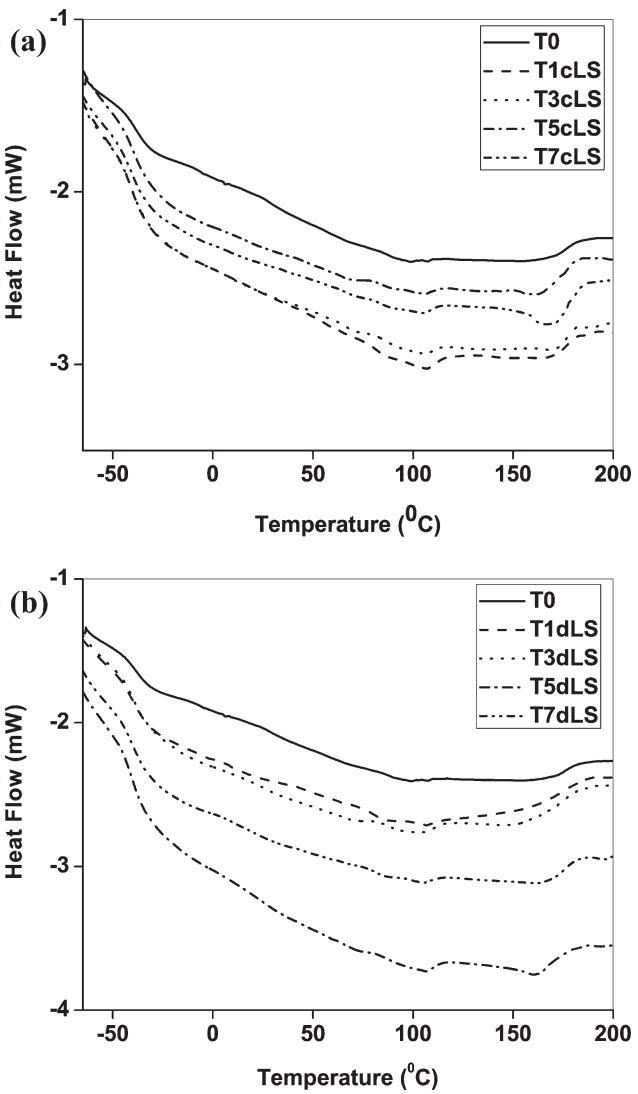

Figure 6 (a) DSC thermogram of TPU and TPUCN with cLS and (b) DSC thermogram of TPU and TPUCN with dLS.

TABLE II
DMA and DSC Results for TPU and TPUCN with cLS and Dls

Sample ID	Storage modulus (Mpa)			tan δ_{max}	T_g	
	−60°C	−20°C	+20°C		DMA	DSC
T0	1587.7	92.0	13.1	0.59	−21.9	−39
T1cLS	3039.6	149.0	26.0	0.55	−24.6	−40
T3cLS	2735.8	145.0	26.1	0.53	−24.5	−40
T5cLS	1772.7	120.4	21.3	0.49	−23.8	−40
T7cLS	1617.4	122.8	20.3	0.46	−23.5	−40
T1dLS	1877.8	108.0	23.8	0.55	−22.0	−40
T3dLS	2800.5	135.82	25.1	0.52	−23.8	−40
T5dLS	3015.3	177.1	29.9	0.49	−23.7	−40
T7dLS	3236.9	208.8	33.0	0.46	−22.0	−40

strain at a frequency of 1 Hz from −80 to 100°C and with a heating rate of 5 °C/min. The values of storage modulus at three different temperatures, the values of tan δ_{max} and T_g are presented in Table II.

Nearly two times increase in storage modulus value is observed for T1cLS when compared with the neat TPU (both in glassy and in rubbery state). In the glassy state, the storage modulus is optimum with 1% clay content and thereafter the modulus gradually decreases with the increase in clay content. A sharp decrease in storage modulus is observed beyond −45°C, which is assumed to be due to the glass-rubber transition of the soft segment. In the rubbery state, storage modulus of the resulting nanocomposite with 1 and 3% cLS is almost two times higher than that of the neat TPU (Table II). However, the value gradually decreases with the increase in clay content. dLS based TPU nanocomposite, however, follows a different trend. In this case, the storage modulus increases monotonously with the increase in clay content. The same trend is observed in both glassy and rubbery states. In the rubbery state nearly 2.5-fold increase in storage modulus is observed with 7% dLS filled composite (Table II).

The decrease in storage modulus value of TPUCN with the increase in cLS content can be ascribed to the increased aggregation and network type of structure formation. The initial increase in storage modulus at lower clay content is due to the balance between intercalation and loose aggregation. However, the increased storage modulus of TPUCN with the increase in dLS content can be ascribed to the preferential association of dLS with the hard segment (as explained earlier) with nearly constant aggregate size for all clay contents. The marginal increase in storage modulus at lower dLS content may be due to the loss of crystalline ordering. The initial loss of crystalline order (due to the penetration of dLS into the hard domain) at lower clay content is compensated largely by the reinforcement due to polymer-filler interaction at higher clay content. This is possible because of the similar size scale of aggregation at lower and higher clay content in this case (refer "Wide angle X-ray diffraction, Transmission electron microscopy, and Field emission scanning electron microscopy" sections).

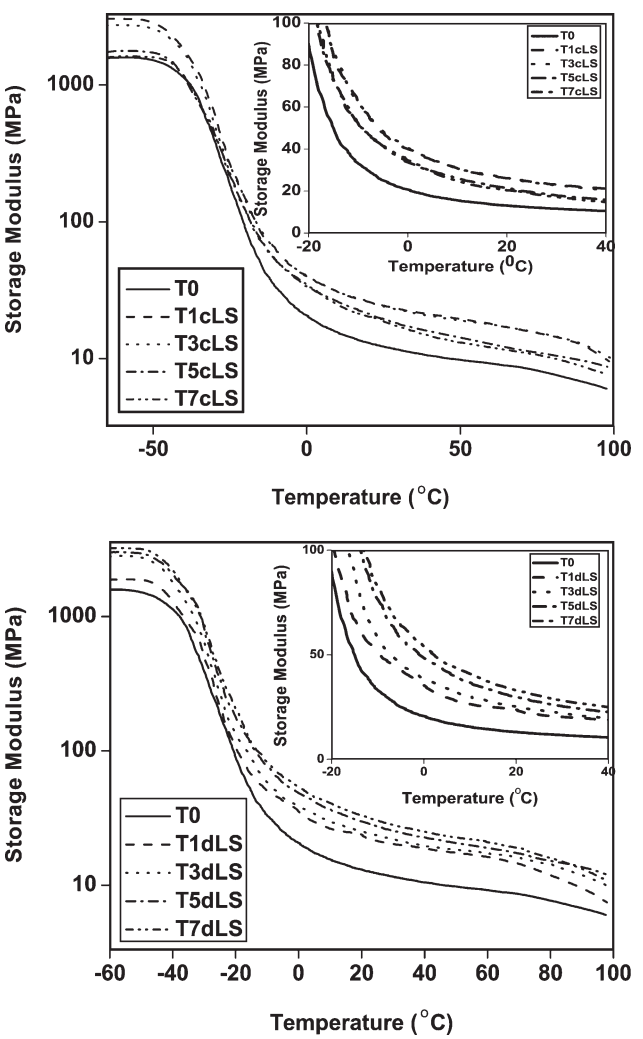

Figure 7 (a) DMA results for TPU and TPUCN with cLS and (b) DMA results for TPU and TPUCN with dLS.

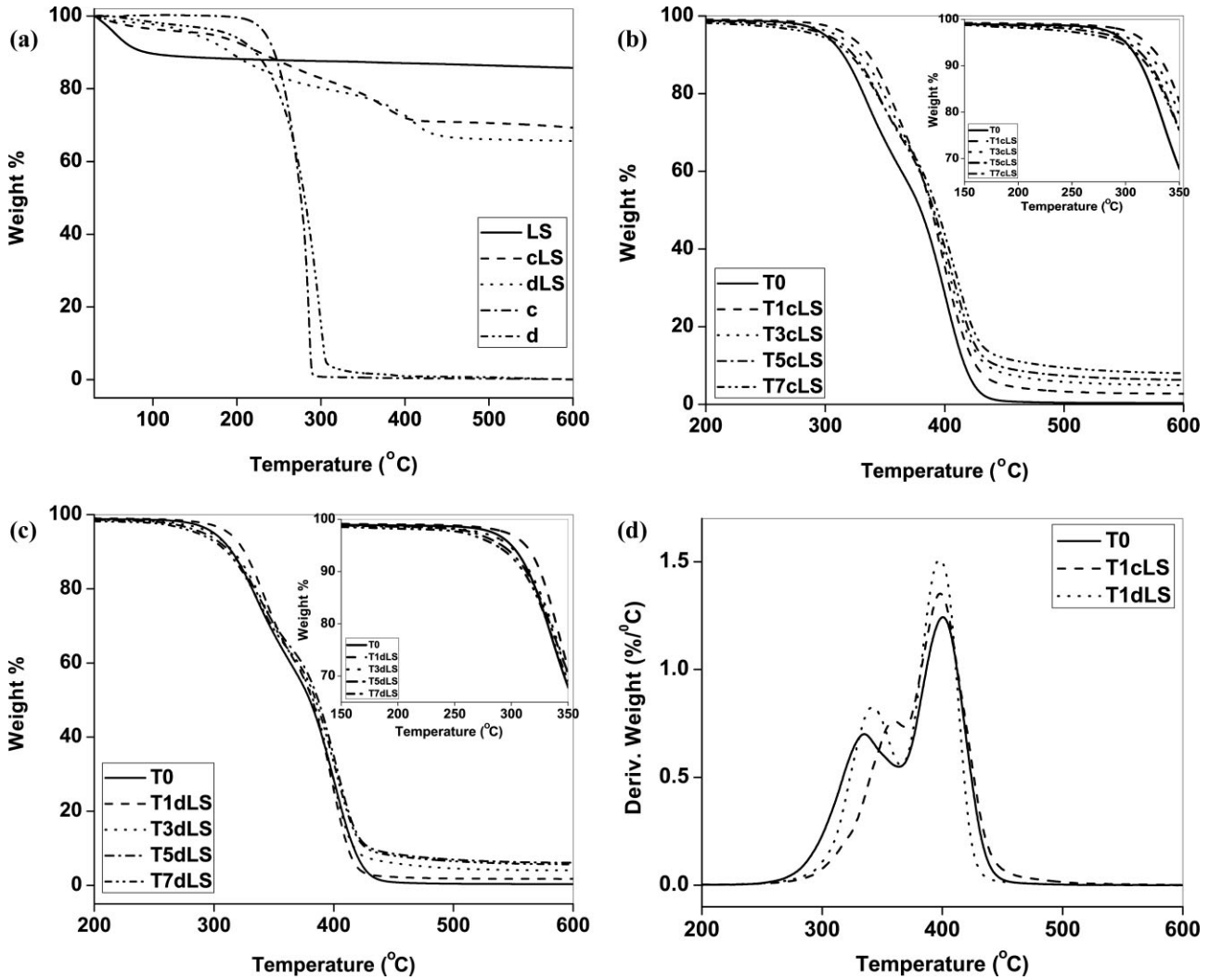

Figure 8 (a) TGA thermogram of amine and surfactants, (b) TGA thermogram of TPU and TPUCN with cLS, (c) TGA thermogram of TPU and TPUCN with dLS, and (d) DTG thermogram of TPU and TPUCN with clS and dLS.

It is observed that the tan δ_{max} value (Table II) gradually decreases with the increase in clay content implying lower damping characteristics. Nearly similar values are observed for cLS and dLS at similar clay content. This is due to the decrease in the fraction of TPU in the nanocomposite with the increase in clay content. Although not much change in T_g is found from DSC, but nearly 2–3°C decrease is observed in DMA. This may be due to the plasticizing effect of a small amount of unreacted amine present inside the clay gallery or due to the segmental dynamics of the polymer inside the clay gallery which become more prominent in dynamic experiments.[22,23]

Thermogravimetric analysis

TGA analysis was carried out in N_2 environment from 40 to 800°C, at a heating rate of 20°C/min. Figure 8(a) displays the TGA thermogram of the unmodified and modified clays. It can be seen that "d" possesses a lower initial thermal stability compared with "c." "d" starts degrading at around 75°C which is possibly due to the removal of HCl and adsorbed moisture but "c" starts degrading at around 175°C. However, above 267°C the thermal stability of "d" is higher than that of "c." The weight loss from 130 to 600°C is due to the loss of alkyl amine group present inside the clay gallery in modified clays. It is observed that modification with "c" and "d" has incorporated 22.5 and 26.4% alkyl amine groups, inside the clay gallery, respectively. When the same modifiers "c" and "d" were used to modify Laponite RD, the percentage of modification were found to be 12.6 and 14.8%, respectively.[15] The increase in nearly 10% weight loss in case of modified Laponite RDS when compared with modified Laponite RD is mainly due to the increase in ion exchange site. The site for additional modification is provided by the sodium pyrophosphate present on

TABLE III
TGA Results for TPU and TPUCN with cLS and dLS

Sample ID	Weight %		
	T_5	T_{1max}	T_{2max}
T0	300	335.1	401.6
T1cLS	319.1 (19.1)	360.0 (24.9)	398.0 (−3.6)
T3cLS	310.1	353.0	398.0
T5cLS	301.5	346.4	404.3
T7cLS	294.5	345.1	407.3
T1dLS	312.5 (12.5)	342.4 (7.3)	397.9 (−3.7)
T3dLS	297.8	341.2	398.1
T5dLS	291.6	336.0	401.2
T7dLS	286.2	336.6	400.4

The values given inside parenthesis indicate the increase in temperature compared with the neat TPU.

the clay surface as explained in the "Introduction" section.

Figure 8(b,c) shows the TGA thermograms of TPUCN with cLS and dLS, respectively. Table III represents the temperature corresponding to the 5% weight loss (T_5), first maximum degradation temperature (T_{1max}), and second maximum degradation temperature (T_{2max}). Although the degradation has started nearly at 200°C (as already mentioned in "Differential scanning calorimetry" section) but to achieve a better comparison (avoiding the weight loss due to the entrapped moisture and unreacted or free amine present inside the clay gallery) comparison is made for 5% weight loss basis.

T_5 is increased by 19.1°C for 1% cLS filled sample (T1cLS) and then it follows a gradual decreasing trend with the increase in clay content. T_{1max} (which is due to the hard segment degradation)[24,25] also follows the same trend and a maximum increase of 25°C is observed with 1% clay filled sample. However, T_{2max} (which is due to the soft segment degradation)[24,25] is lower than that of neat TPU up to 3% cLS content. T_{2max} becomes higher than neat TPU for >5% clay content. T_{2max} follows an increasing trend with the increase in clay content, unlike with T_{1max}. Similar trend is followed for T_5, T_{1max}, and T_{2max} in case of dLS based TPUCN as well. A 12.5°C and 7.3°C increase in T_i and T_{1max} is observed with 1% dLS content when compared with the neat TPU. However, in dLS based TPUCN, T_{2max} values are always less than that of the neat TPU.

The decrease in T_5, with an increase in clay content in both the cases is due to the presence of excess/unreacted amine left over inside the clay gallery.[15] Because of the presence of greater amount of surfactant in dLS compared with cLS (as mentioned earlier), T_{1max} value of cLS based TPUCN is higher than that of dLS based TPUCN. The decrease in T_{2max} value when compared with the pure TPU reflects the hard segment preference of Laponite RDS. In our earlier work, it was observed that when modified Laponite RD was associated with the soft segment,[14] T_{2max} was higher than that of neat TPU. However, when it was associated with the hard segment,[15] T_{2max} was lower than that of neat TPU. A comparative study shows that, there is not much change in T_{2max} value (Table III) for the composites having lower cLS and dLS content. However, T_{2max} value for T7cLS is 7°C higher than that of T7dLS. This is possible only because of the network structure (distributed both in hard and soft segment) formed by cLS at higher clay content. However, due to the confined structure of dLS at the vicinity of hard segments, it is unable to interfere with degradation process of the soft segment.

Isothermal TGA

Both isothermal and dynamic methods are used[26–29] to calculate the activation energy of degradation for unfilled and filled polymeric systems. An attempt is made in this work to carefully look into the effect of modifier on the degradation behavior of TPUCN under isothermal conditions. For this study, three different temperatures (300, 325, and 350°C) were selected based on the degradation behavior of TPU via dynamic TGA experiment ("Thermogravimetric analysis" section). Figure 9 shows the isothermal TGA thermogram of T0, T1cLS, and T1dLS at different temperatures. The nanocomposites are represented here in as T*xy*_*z*, where, *z* represents the corresponding temperatures at which isothermal experiment is carried out. Mechanisms of degradation of TPU are shown in Scheme 1. In absence of any external stimuli it is expected to follow a first order rate equation and the equation is represented as follows:

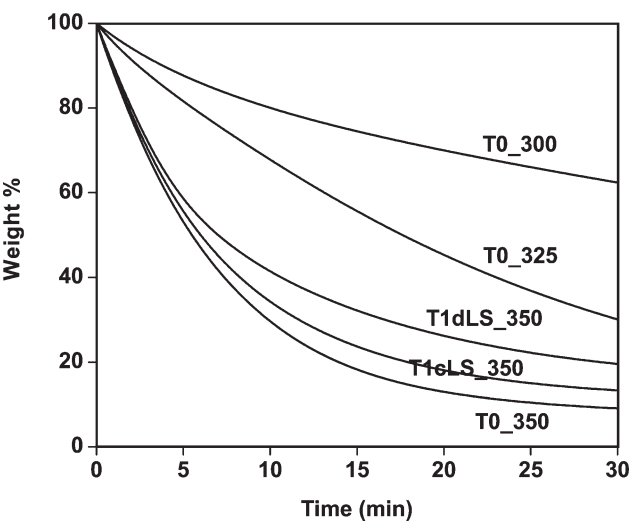

Figure 9 Isothermal TGA thermogram for T0, T1cLS, and T1dLS at 300, 325, and 350°C.

$$\ln C = -kt + \ln C_0 \quad (2)$$

or

$$\ln(C/C_0) = -kt \quad (3)$$

A plot of ln (C/C_0) versus t is expected to result a straight line passing through origin with a slope of $-k$. In this case, C is the weight after time t, C_0 is the initial weight, and k is the rate constant.

The increase in k value at higher temperatures indicates the increased rate of degradation with the increase in temperature.

According to Arrhenius equation

$$k = Ae^{-E/RT} \quad (4)$$

or

$$\ln k = \ln A - E/RT \quad (5)$$

Hence, the plot of ln k versus $1/T$ results in a straight line with a slope of $-E/R$, where, "E" is the activation energy, "R" the universal gas constant (8.314 J/(mol K)), "T" the absolute temperature, and "A" is the pre-exponential factor. From the slope, activation energy E can be calculated. The rate constants and activation energy of neat TPU, T1cLS, and T1dLS were calculated and compared in Table IV.

Isothermal degradation process is mostly contributed by two factors: polymer decomposition and physical stabilization. It is observed that at 300°C, the rate constant "k" remain indifferent for neat TPU, T1cLS, and T1dLS. At 325°C, k value of neat TPU is marginally higher than that of T1cLS and T1dLS (k value remaining indifferent for both T1cLS and T1dLS). However, at 350°C, k value follows the order T1cLS < T1dLS < T0 (Table IV). In all the three cases, k value increases with the increase in temperature (i.e., k value follows the order 300 < 325 < 350). From the k values, it is quite obvious that T1cLS is providing better thermal stability to TPU. Although the same is not reflected at lower temperatures but it is quite clear at 350°C.

However, the activation energy follows the order T0 > T1dLS > T1cLS. As observed in earlier section, thermal stability follows the order T0 < T1dLS < T1cLS, which is just the reverse of the trend in activation energy found here. To confirm the decrease in activation energy with the addition of modified clay, several other TPU-clay nanocomposites (based on commercially available modified Cloisite 20A and Laponite RD modified by "c" and "d") were prepared and the same isothermal experiment was conducted (the results will be communicated separately). In all the cases, the activation energy is found to decrease when compared with the neat TPU although an increase in thermal stability is observed by TGA with the dynamic temperature ramp. Similar results are reported recently by Fambri et al.[28] by following the similar technique. The increase in thermal stability is due to the nonconducting barrier effect of inorganic clay platelets. Although the exact reason for the decrease in activation energy is not known but there may be two reasons as follows: (i) one may be due to the complex mechanism followed at different temperatures (as already mentioned in the "Introduction" section that degradation of TPU follows a complex mechanism) and (ii) the second may be due to the contribution of the initial thermal history (10°C ramp from room temperature to 300, 325, and 350°C).

TABLE IV
Rate Constants at Different Isothermal Degradations

Sample ID	k (s^{-1}) $\times 10^{-3}$ at 300°C	k (s^{-1}) $\times 10^{-3}$ at 325°C	k (s^{-1}) $\times 10^{-3}$ at 350°C	Activation energy (J)
T0	0.3 (0.95)	0.7 (1.00)	1.5 (0.92)	95.54
T1cLS	0.3 (0.97)	0.6 (0.98)	1.0 (0.91)	71.58
T1dLS	0.3 (0.93)	0.6 (1.00)	1.3 (0.90)	86.92

The values given inside parenthesis indicate the correlation coefficient.

CONCLUSION

Laponite RDS is modified successfully with two different surfactants (cetyltrimethyl ammonium bromide and dodecylamine hydrochloride) and dispersed in TPU matrix by solution mixing technique. Morphology of these two modified clay-nanocomposites is markedly different from each other. cLS based TPU nanocomposites exhibit partly exfoliated, intercalated, and aggregated structure at lower clay content, but a network type of structure at higher clay content is observed. However, dLS based TPU nanocomposites exhibit spherical cluster type of structure at all clay contents studied. Nearly two fold increase in storage modulus is observed in both glassy and rubbery state with merely 1% cLS addition, but gradually it decreases with an increase in clay content. However, in case of dLS filled nanocomposite, gradual increase in storage modulus is observed with the increase in clay content. Thermal stability of the nanocomposite (for 5% weight loss) is improved by 19.1 and 12.5°C when compared with the neat TPU, with only 1% addition of cLS and dLS, respectively. The isothermal degradation process was used to calculate the rate constants and

activation energy at different temperatures. Although thermal stability follows the order T0 < T1dLS < T1cLS but activation energy follows the reverse trend.

The authors thank Mr. T. K. Mallik of M/S Bayer Materials Science Pvt. Ltd., Chennai for supplying Desmopan KU2 8600E. The cooperation and encouragement received from Mr. M. A. Joseph, the response coordinator, Dr. V. L. Rao, the focal scientist, and Dr. K. N. Kinan, the Group Director of Propellant and Chemical group, VSSC, Trivandrum is gratefully acknowledged.

References

1. Song, L.; Hu, Y.; Tang, Y.; Zhang, R.; Chen, Z.; Fan, W. Polym Degrad Stab 2005, 87, 111.
2. Woo, J. C.; Kim, S. H.; Kim, Y. J. Polymer 2004, 45, 6045.
3. Pattanayak, A.; Jana, S. C. Polym Eng Sci 2005, 45, 1532.
4. Jiang, H.; Qian, J.; Bai, Y.; Fang, M.; Qian, X. Polym Compos 2006, 27, 470.
5. Rehab, A.; Akelah, A.; Agag, T.; Shalaby, N. Polym Compos 2007, 28, 108.
6. Pan, Q.; Zou, H.; Wu, S.; Shen, J. Polym Compos 2008, 29, 119.
7. Zou, H.; Ran, Q.; Wu, S.; Shen, J. Polym Compos 2008, 29, 385.
8. Saunders, J. H.; Frisch, K. C. Polyurethane: Chemistry and Technology; Wiley-Interscience: New York, 1962; Part 1, pp 106–121.
9. Rumao, P. L.; Frisch, K. C. J Polym Sci A1 1972, 10, 1499.
10. Rapp, N. S.; Ingham, D. J. J Polym Sci A2 1964, 689, 4941.
11. Matuszak, M. L.; Frisch, K. C. J Polym Sci Part B: Polym Chem Ed 1973, 11, 637.
12. Mishra, A. K.; Chattopadhyay, S.; Nando, G. B.; Devadoss, E. Design Monom Polym 2008, 11, 395.
13. Mishra, A. K.; Nando, G. B.; Chattopadhyay, S. J Polym Sci Part B: Polym Phys 2008, 46, 2341.
14. Balnois, E.; Durand-Vidal, S.; Levitz, P. Langmuir 2003, 19, 6633.
15. Rosta, L.; von Gunten, H. R. J Colloid Interface Sci 1990, 134, 397.
16. Wheeler, P. A.; Wang, J.; Baker, J.; Mathias, L. J. Chem Mater 2005, 17, 3012.
17. Liff, S. M.; Kumar, N.; McKinley, G. H. Nat Mater 2007, 6, 76.
18. Chen, T. K.; Shieh, T. S.; Chui, J. Y. Macromolecules 1998, 31, 1312.
19. Tsen, W. C.; Chuang, F. S. J Appl Polym Sci 2006, 101, 4242.
20. Seymour, R. W.; Cooper, S. L. Macromolecules 1973, 6, 48.
21. Shu, Y. C.; Lin, M. F.; Tsen, W. C.; Chuang, F. S. J Appl Polym Sci 2001, 81, 3489.
22. Xiong, J.; Liu, Y.; Yang, X.; Wang, X. Polym Degrad Stab 2004, 86, 549.
23. Anastasiadis, S. H.; Karatasos, K.; Vlachos, G.; Manias, E.; Giannelis, E. P. Phys Rev Lett 2000, 84, 915.
24. Petrovic, Z. S.; Zavargo, Z.; Flynn, J. F.; Macknight, W. J. J Appl Polym Sci 1994, 51, 1087.
25. Shieh, Y. T.; Chen, H. T.; Liu, K. H.; Twu, Y. K. J Polym Sci Part A: Polym Chem 1999, 37, 4126.
26. Lu, M. G.; Lee, J. Y.; Shim, M. J.; Kim, S. W. J Appl Polym Sci 2002, 85, 2552.
27. Zonga, R.; Hua, Y.; Wang, S.; Songa, L. Polym Degrad Stab 2004, 83, 423.
28. Fambri, L.; Pegoretti, A.; Gavazza, C.; Penati, A. J Appl Polym Sci 2001, 81, 1216.
29. Nam, J. D.; Seferis, J. C. J Polym Sci Part B: Polym Phys 1992, 30, 455.